Optical and magnetic properties induced by structural confinement of ternary chalcogenide in SBA-15 nanotube

J.-S. Jung and K.-H. Choi
Department of Chemistry, Kangnung National University, Kangnung 210-702, South Korea

Y.-R. Kim, W.-S. Chae, and S.-H. Lee
Department of Chemistry, Yonsei University, Seoul 120-749, South Korea

L. Malkinski,[a] V. Golub, and C. J. O'Connor
Advanced Materials Research Institute, University of New Orleans, New Orleans, Louisiana 70148

(Presented on 12 November 2002)

The amorphous ternary material, $Ni_3(SbTe_3)_2$ was prepared using a rapid precipitation reaction between the Zintl phase K_3SbTe_3 and $NiBr_2$ in solution. This material induced by the incorporation of ternary chalcogenide into long range ordered mesoporous SBA-15 was transformed into ternary nanoparticles. Structural confinement of the amorphous ternary chalcogenide in the mesoporous silica tube causes the suppression of phonon coupling to photoexcited carriers in the confined ternary chalcogenide, resulting in narrower photoluminescence (PL) band than those of the bulk ternary chalcogenide. It also gives rise to ferromagnetic behavior of the nanoparticles made from the material, which is a spin glass with the freezing temperature of 4.0 K in a bulk form. The physical and chemical properties of obtained ternary bulk and nanoparticles have been investigated by x-ray diffraction, superconducting quantum interference device, transmission electron microscopy, Brunauer–Emmett–Teller, and PL (steady-state photoluminescence spectroscopy). The role played by the modified SBA-15 porous silica in controlling ternary chalcogenide size and quantities has been discussed. © *2003 American Institute of Physics.* [DOI: 10.1063/1.1558202]

I. INTRODUCTION

We have reported a room temperature chemical route to the amorphous alloys $M_3(SbTe_3)_2$ (M=Cr, Mn, Fe, Co, Ni) where it was shown that the trigonal $SbTe_3$ unit present in the K_3SbTe_3 starting material was structurally intact in the amorphous M_3SbTe_3.[1–3] The amorphous nature of the product is due to the very rapid precipitation reaction and corresponding magnetic structure exhibited spin-glass behavior at the low temperature.[4] Despite the wealth of the electric and magnetic properties of these amorphous materials, little is being done to explore the physical properties of the confined nanostructure.[5–7] Recently amorphous ternary compound of $Ni_3(SbTe_3)_2$ and its nanostructured equivalent within the AlMCM41 host have been studied using spectroscopic tools.[8] This regular pore structure of AlMCM41 offered a suitable reaction chamber for the controlled assembly of nanostructured materials, but the smaller pore size of AlMCM41 limited the insertion of $Ni_3(SbTe_3)_2$. The SBA15 host with larger pore diameter provides much better reaction template for nanostructured ternary compound. The host material with well-ordered hexagonal honeycomb array prevents particle aggregation[9] and is a template for the isolated nanostructured material. In the present study, we employed mesoporous AlSBA15 as a host material in the preparation of confined nanostructured ternary chalcogenide compound and investigated in terms of its interesting optical and magnetic properties.

II. EXPERIMENTAL SECTION

The ternary Zintl material and the transition-metal compound $Ni_3(SbTe_3)_2$ were prepared as described previously.[1,2] Due to the extreme sensitivity of these compounds, all manipulations were carried out in an argon-filled glovebox containing less than 1 ppm of oxygen. The synthesis process of $Ni_3(SbTe_3)_2$–AlSBA15 was conducted in Schlenk tubes equipped with magnetic stirring bars and was held under pure Ar gas. AlSBA15 (0.5 g)[10] was slowly stirred in 30 ml of 0.05 M $NiBr_2$ aqueous solution. To remove the outer surface of the host channel, the resulting Ni^{2+}–AlSBA15 gray powder was suspended and repeatedly washed in distilled water. The addition of K_3SbTe_3 solution into the Ni^{2+}–AlSBA15 resulted in the final black powdered form of the nanocomposites, the $Ni_3(SbTe_3)_2$ incorporated in AlSBA15.

A Quantum Design MPMS-5S superconducting quantum interference device magnetometer was used for the magnetic measurements. A general discussion on magnetic susceptibility measurements and the calibration techniques have been described in details elsewhere.[11] Transmission electron microscopy (TEM) imaging was performed on a JEOL 3010 transmission electron microscope. Powder x-ray diffraction (XRD) data were collected on a Philips X'Pert MPD system equipped with copper radiation ($\lambda = 1.5418$ Å) and a graphite monochromer. Steady-state photoluminescence (PL) and photoluminescence excitation (PLE) spectra were measured with a fluorimeter (Hitachi F-4500).

---
[a] Authors to whom correspondence should be addressed; electronic mail: iiscm@kangnung.ac.kr. and lmalkins@uno.edu
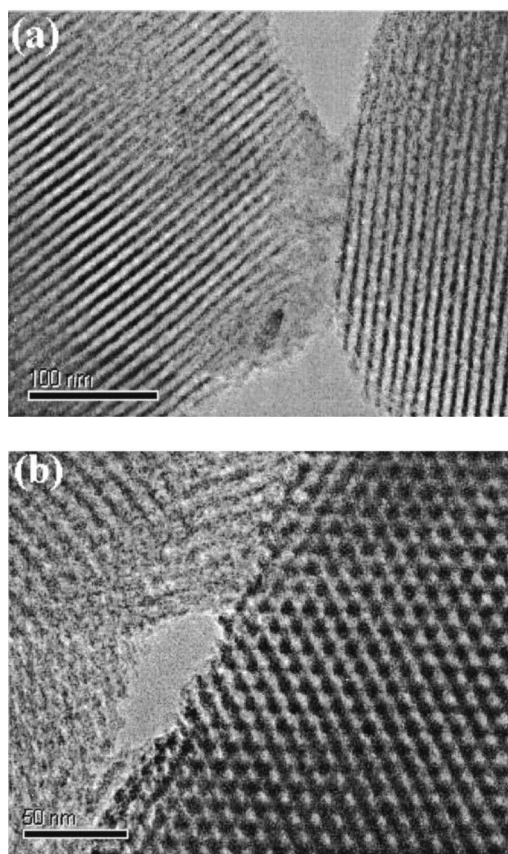
J. Appl. Phys., Vol. 93, No. 10, Parts 2 & 3, 15 May 2003

Jung *et al.* 6955

FIG. 1. TEM images of $Ni_3(SbTe_3)_2$–AlSBA15 (a) lamellar structure from a projection of a hexagonal array of tubules and (b) hexagonal pore structure.

FIG. 3. PL (solid line) and PLE (dashed line) spectra at room temperature: (a) bulk $Ni_3(SbTe_3)_2$ and (b) $Ni_3(SbTe_3)_2$–AlSBA15. λ_{ex} and λ_{em} represent an excitation wavelength for PL spectrum and a detection wavelength for PLE spectrum, respectively.

III. RESULTS AND DISCUSSION

The TEM images of incorporated structure of $Ni_3(SbTe_3)_2$ in AlSBA15 mesopore confirm the conservation of initial long-range ordered porous structure, without bulk $Ni_3(SbTe_3)_2$ particles outside of the host channels (Fig. 1). The energy dispersive x-ray analysis confirms the existence of $Ni_3(SbTe_3)_2$ in nanocomposites, although we did not iso-

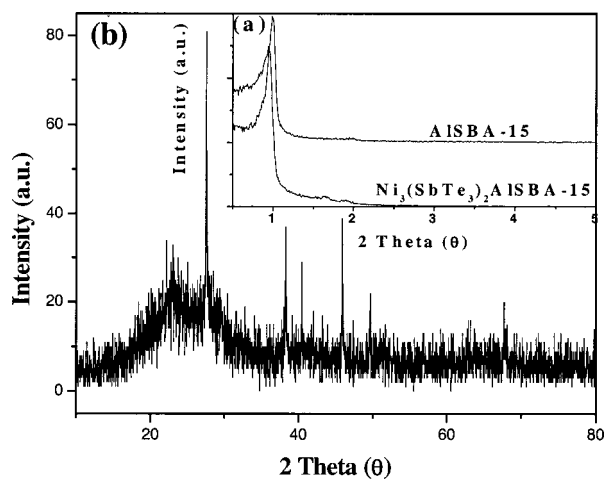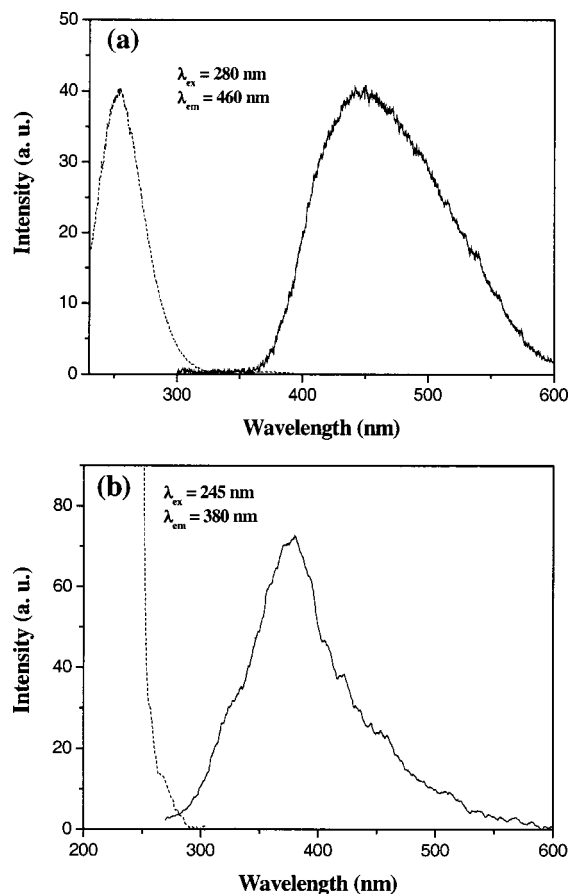FIG. 2. (a) XRD patterns at low angles $Ni_3(SbTe_3)_2$–AlSBA15 and pure AlSBA15 and (b) XRD pattern at high angles for $Ni_3(SbTe_3)_2$–AlSBA15.

late the image of ternary compound itself. The similar imaging effect has also been reported in the case of $Ni_3(SbTe_3)_2$ clusters impregnated in mesoporous AlMCM41.[8] XRD patterns at low angles of $Ni_3(SbTe_3)_2$–AlSBA15 and pure AlSBA15 are presented in Fig. 2(a). The d_{100} peak of the $Ni_3(SbTe_3)_2$ incorporated in AlSBA15 shifts slightly to a lower angle [from $2\theta = 0.99$ for pure AlSBA15 to $2\theta = 0.95$ for $Ni_3(SbTe_3)_2$–AlSBA15]. This is due to a slight expansion of the mesopores in AlSBA15 caused by the insertion of the $Ni_3(SbTe_3)_2$ into the host. The XRD pattern of $Ni_3(SbTe_3)_2$–AlSBA15 at high angles shows the same diffraction peaks as $Ni_3(SbTe_3)_2$–AlMCM41,[8] while both the host (AlSBA15) and the amorphous bulk $Ni_3(SbTe_3)_2$ show only broad diffraction in same angle region.[12] The average crystallite size, as could be calculated from line broadening at 27.5°, was 65 nm. It suggests that the particles exist not in a spherical form but in an elongated morphology because pore size of AlSBA15 is less than 5.5 nm.

The ternary chalcogenide structurally confined in AlSBA15 shows excitation spectrum onset at ~ 290 nm and emission spectrum centered at ~ 380 nm (Fig. 3). Since the observed emission spectrum is largely Stokes shifted from the excitation onset, the emission is ascribed to exciton recombination through deeply trapped states after light absorption, as in the case of the similar emission characteristics for
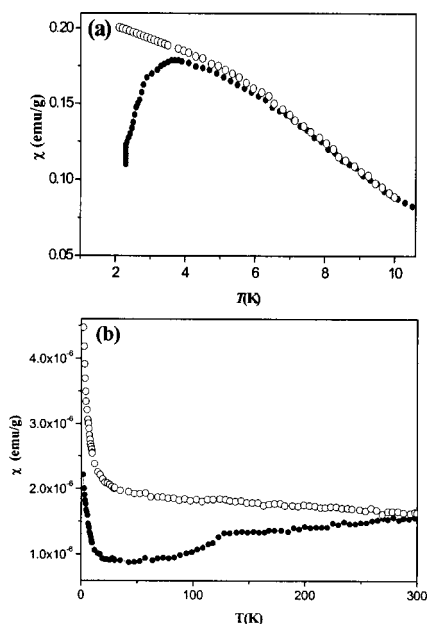
FIG. 4. (a) Temperature dependent FC (empty circle) and ZFC (filled circle) dc magnetic susceptibilities for the bulk $Ni_3(SbTe_3)_2$, and (b) temperature dependent FC (empty circle) and ZFC (filled circle) dc magnetic susceptibilities for $Ni_3(SbTe_3)_2 - AlSBA15$.

FIG. 5. Hysteresis loops of $Ni_3(SbTe_3)_2 - AlSBA15$ at 300 K.

ternary chalcogenide confined in AlMCM41.[8] When $Ni_3(SbTe_3)_2$ ternary chalcogenide is incorporated into mesoporous AlSBA15, excitation spectrum onset is blueshifted (from ~320 to ~290 nm) and emission spectrum is also blueshifted from those of the bulk chalcogenide (from ~450 to ~380 nm). Such results are probably due to quantum confinement effect, since the incorporated ternary chalcogenide has somewhat discrete nanodomain in the mesoporous AlSBA15 nanochannels.

In addition to magnetooptical properties the dimensional confinement also affects magnetic properties. The magnetic properties of the bulk $Ni_3(SbTe_3)_2$ compound are characteristic of spin glasses. Frustration of magnetic moments in spin glasses gives rise to susceptibility dependence on temperature presented in Fig. 4(a). Different magnetic moment distributions are "frozen" when spin glass is cooled below so called "freezing temperature" (T_f) in the presence or in the absence of external magnetic field. The susceptibility curves converge only above $T_f = 4$ K when multiple energy states are available for thermally excited frustrated spins. In contrast the nanosized particles of the $Ni_3(SbTe_3)_2$ material grown in the AlSBA15 show distinctly different magnetic behavior from the bulk material. First of all, the susceptibility [Fig. 4(b)] and magnetization loops (Fig. 5) are charac-
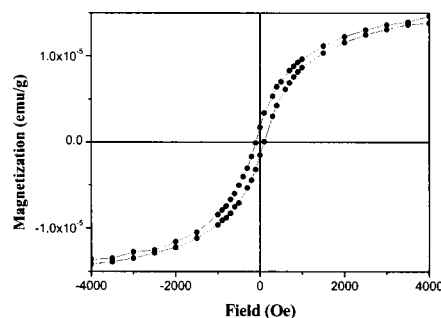
teristic of ferromagnetic material rather than of a spin glass. It is important to notice that spin-glass structure requires specific spin arrangement and in very small particles this condition may not be satisfied for relatively large number of spins at the particle surface resulting in ferromagnetic instead of spin-glass behavior. Because of very elongated shape of the particles (length > 60 nm) and possible magnetostatic interactions among particles the blocking temperature of the superparamagnetic particles is expected to be above room temperature, which explains the magnetic hysteresis at room temperature and split of susceptibility curves below room temperature. Complete understanding of the magnetic behavior of nanoparticles of spin glass materials is a complex problem because of overlapping of spin-glass and superparamagnetic properties.

ACKNOWLEDGMENT

[1] J.-S. Jung, E. D. Stevens, and C. J. O'Connor, J. Solid State Chem. **94**, 362 (1991).
[2] J.-S. Jung, L. Ren, and C. J. O'Connor, J. Mater. Chem. **2**, 829 (1992).
[3] J.-S. Jung, B. Wu, J. Tang, J. Jamet, and C. J. O'Connor, J. Mater. Res. **9**, 909 (1994).
[4] C. J. O'Connor, J.-S. Jung, J. H. Zhang, in *Chemistry, Structure, and Bonding of Zintl Phases and Ions*, edited by S. M. Kauzlarich (VCH, New York, 1996).
[5] J.-S. Jung, H. H. Kim, S. G. Kang, J. H. Jun, L. Ren, and C. J. O'Connor, Inorg. Chim. Acta **268**, 271 (1998).
[6] R. C. Haushalter, C. J. O'Connor, J. P. Haushalter, A. M. Umarji, and G. K. Shenoy, Angew. Chem. **97**, 147 (1984).
[7] J.-S. Jung, B. Wu, L. Ren, and C. J. O'Connor, J. Appl. Phys. **73**, 5463 (1993).
[8] W.-S. Chae, I.-W. Hwang, J.-S. Jung, and Y.-R. Kim, Chem. Phys. Lett. **341**, 279 (2001).
[9] J. S. Beck *et al.*, J. Am. Chem. Soc. **114**, 10834 (1992).
[10] D. Zhao, J. Feng, Q. Huo, N. Melosh, G. H. Fredrickson, B. F. Chmelka, and G. D. Stucky, Science **279**, 548 (1998).
[11] C. J. O'Connor, Prog. Inorg. Chem. **29**, 203 (1982).
[12] W.-S. Chae, J.-S. Jung, and Y.-R. Kim, J. Phys. Chem. B **107**, 1585 (2003).